Acta Biochimica Polonica

Vol. 53 No. 1/2006, 113–120

on-line at: www.actabp.pl

Regular paper

The influence of modification at position 2 on the side-chain conformation in oxytocin analogs

Bogusław Śmiech✉, Rajmund Kaźmierkiewicz and Bernard Lammek

Faculty of Chemistry, University of Gdańsk, Gdańsk, Poland; ✉e-mail: bogus@chem.univ.gda.pl

Received: 25 May, 2005; revised: 19 December, 2005; accepted: 23 January, 2006
available on-line: 07 March, 2006

The nonapeptide oxytocin (OT) is used in medicine to help begin and/or continue childbirth. Its analogs can be also used to control bleeding following fetus delivery. The main function of oxytocin is to stimulate contraction of uterus smooth muscle and the smooth muscle of mammary glands, thus regulating lactation. This paper describes theoretical simulations of the distribution of the torsional angles $\chi 1$ in the non-standard methylated phenylalanine residues of three oxytocin analogs: [(Phe)^2*o*-Me]OT, [(Phe)^2*m*-Me]OT, [(Phe)^2*p*-Me]OT. The conformations of the oxytocin analogs were studied both in vacuum and in solution. We found some correlations between the biological activity of the considered peptides and the side-chain conformations of amino-acid residues 2 and 8.

Keywords: oxytocin analogs, torsional angle distribution, EDMC

Currently, preterm birth is fairly frequent (about 10% of all births in USA) (Wyatt *et al.*, 2001) and remains the main cause of neonatal mortality and morbidity. On the other hand, prolonged retardation of labor can be dangerous for the fetus health and life. Therefore studying novel, effective tools for controlling parturition is of utmost importance. Searching among analogs of the natural hormone oxytocin, involved in childbirth seems reasonable approach. Oxytocin is a nonapeptide involved in the induction of labor by stimulating uterine smooth muscle contractions and in stimulation of the milk ejection by mammary gland and of specific sexual, affiliative and maternal behaviors. The hormone and its analogs are used in medicine to help begin and/or continue childbirth or to control bleeding following fetus delivery. Oxytocin is produced in the supraoptic and paraventricular nuclei in the hypothalamus and is released to blood by posterior pituary gland. Human oxytocin has the following sequence:

H-Cys-Tyr-Ile-Gln-Asn-Cys-Pro-Leu-Gly-NH_2

Oxytocin initiates its physiological activity by interacting with the G-protein-coupled receptor (GPCR) known as oxytocin receptor (OTR). All members of GPCR superfamily, including OTR, consist of seven hydrophobic transmembranes-helices joined by alternating intra- and extracellular loops (Barberis *et al.*, 1998). Since the work of Law and Vigneaud in 1960 (Law & Vigneaud, 1960) a large number of oxytocin analogs have been synthesized and many have been reported as oxytocin agonists or antagonists often more potent than the natural hormone (Toth *et al.*, 1999). Nevertheless, no fully medical agents are available at present to treat woman in preterm labor. This is so mainly because of the low orall activity or undesirable maternal or neonatal side effects of the synthesized analogs (Higby & Suiter, 1999). Therefore a research for new effective antagonists blocking oxytocin receptor and preventing preterm labor appears necessary. It is believed the critical role in the agonistic–antagonistic properties of the neurohormon analogs is played by amino-acid residues in position 2 and 8 (Bankowski *et al.*, 1980; Manning *et al.*, 1984; 1995; Hruby *et al.*, 1994). Therefore main modifications concern these positions. In this work we investigated the structure of oxytocin analogs modified at the second position: [(Phe)^2*o*-Me]OT, [(Phe)^2*m*-Me]OT, [(Phe)^2*p*-Me]OT. Their interesting feature is the difference in the ago-

Abbreviations: GPCR, G-protein-coupled receptor; ECEPP, empirical conformational energy program for peptides; EDMC, electrostatic driven Monte Carlo; OT, oxytocin; OTR, oxytocin receptor.

nistic and antagonistic properties which depends on the site of the methyl group substitution in the phenyl ring of phenylalanine. Their activity also strongly depends on the presence of magnesium ions. In their absence oxytocin analogs containing the *ortho* and *meta* isomer are antagonists, while that containing the *para* isomer is an agonist. In the presence of magnesium ions the peptide containing the *meta* isomer shows antagonistic activity, while the analogs with the *ortho* and *para* isomers are agonists (Slaninova *et al.*, 2001). Oxytocin contains a ring created by six amino-acid residues connected by a disulfide bond between residues Cys^1 and Cys^6, and a "tail" of three amino-acid residues. Structural studies of oxytocin and its analogs (Urry *et al.*, 1970; Wood *et al.*, 1986; Budesinsky *et al.*, 2005) reveal high flexibility of the "tail" and low flexibility of the peptide ring stabilized by two H-bonds. The relatively rigid ring serves as a frame for the amino-acid side chains, whose spatial arrangement is believed to play a crucial role in the peptide–receptor interactions. The torsional angle $\chi 1$ describes rotation around the C_α–C_β bond in amino-acid residues and changes of the $\chi 1$ value have a significant influence on the conformation of a particular side chain. The main goal of this paper was to obtain the distributions of the dihedral angle $\chi 1$ values using various theoretical methods, including quantum mechanics and semiemipirical methods at the setup level, with molecular mechanics playing the leading role. The conformations of oxytocin analogs were studied both in vacuum and in solution.

METHODS

The ECEPP/3 (Burgess *et al.*, 1975; Nemethy *et al.*, 1983; 1992) force field was used to generate a set of several thousand structures of [(Phe)^2*o*-Me]OT, [(Phe)^2*m*-Me]OT and [(Phe)^2*p*-Me]OT using the elec-

Table 1. Z-matrix with charges for nonstandard residue *o*-Me-Phe introduced to ECEPP/3 database

Atom		Bond		Angle		Dihedral	Charge
N	1						–0.60798
HN	1	1.000					0.29423
CA	1	1.453	2	114.999			0.00804
HA	3	1.090	1	107.265	2	119.4	0.11501
CB	3	1.530	1	106.999	2	–118.8	–0.07839
C	3	1.530	1	111.000	2	0.0	0.07524
O	6	1.230	3	120.500	1	0.0	0.09663
HB	5	1.090	3	108.910	1	–58.2	–0.05192
HB	5	1.090	3	108.905	1	58.2	0.12109
CG	5	1.530	3	113.999	1	180.0	–0.20301
CD1	10	1.360	5	119.999	3	180.0	0.06220
CD2	10	1.360	5	120.003	3	0.0	0.08380
CE1	11	1.420	0	119.998	5	180.0	0.06636
CE2	12	1.420	0	120.003	5	180.0	–0.17203
HD2	12	1.090	0	119.997	5	0.0	0.13541
HE1	13	1.090	1	119.999	10	180.0	–0.16631
CZ	13	1.360	1	120.003	10	0.0	0.14541
HE2	14	1.090	2	120.002	10	180.0	–0.12652
HZ	17	1.090	3	120.007	11	180.0	0.13258
CK	11	1.450	0	119.968	5	–0.1	–0.18503
HK	20	1.089	11	109.485	10	0.0	0.15138
HK	20	1.089	11	109.452	10	120.0	0.51784
HK	20	1.089	11	109.484	10	–120	–0.41403

Table 2. Z–matrix with charges for nonstandard residue *m*-Me-Phe introduced to ECEPP/3 database

Atom		Bond		Angle		Dihedral	Charge
N	1						–0.60798
HN	1	1.000					0.29423
CA	1	1.453	2	114.999			0.00804
HA	3	1.090	1	107.265	2	119.4	0.11501
CB	3	1.530	1	106.999	2	–118.8	–0.07839
C	3	1.530	1	111.000	2	0.0	0.07524
O	6	1.230	3	120.500	1	0.0	0.09663
HB	5	1.090	3	108.910	1	–58.2	–0.05192
HB	5	1.090	3	108.905	1	58.2	0.12109
CG	5	1.530	3	113.999	1	180.0	–0.17203
CD1	10	1.360	5	119.999	3	180.0	–0.03680
CD2	10	1.360	5	120.003	3	0.0	–0.20301
HD1	11	1.090	10	120.000	5	0.0	–0.16631
CE1	11	1.420	10	119.998	5	180.0	0.14541
CE2	12	1.420	10	120.003	5	180.0	–0.12652
HD2	12	1.090	10	119.997	5	0.0	0.13258
CK	14	1.451	11	119.954	10	180.0	–0.18503
CZ	14	1.360	11	120.003	10	0.0	0.15138
HE2	15	1.090	12	120.002	10	180.0	0.06220
HK	17	1.088	14	109.513	11	0.1	0.08380
HK	17	1.089	14	109.392	11	120.0	0.06636
HK	17	1.089	14	109.510	11	–120.0	0.51784
HZ	18	1.090	14	120.007	11	180.0	–0.41403

trostatically driven Monte Carlo method (EDMC). A great number of structures of the examined peptides were needed, which could be obtained in two ways: through molecular dynamics (e.g. using AMBER package (Pearlman *et al.*, 1995)) or through the EDMC method implemented in ECEPP force field. We regard the EDMC method as superior in searching the conformational space in comparison to the high-temperature molecular dynamics. We decided to use the EDMC method, which being stochastic, was more suitable for our purpose. We needed tools for the production of as many as possible different conformations forming the statistical population of the peptides. The nonstandard residues geometry was created using phenylalanine structure from the ECEPP/3 database as a template by simple substitution of a hydrogen atom by the methyl group in the phenyl ring. These modifications were performed using the program Molden (Schaftenaar & Noordik, 2000). The distribution of charges on the nonstandard residue atoms was taken from the Mopac calculations using MNDO/3 method (Bingham *et al.*, 1975). Partial atomic charges were obtained by fitting point charges to the MNDO electrostatic potential. It is the standard procedure of developing new residues in the ECEPP/3 force field. Tables 1, 2 and 3 (in the z-matrix form) include partial atomic charges multiplied by factor $\sqrt{322.0/2.0}$ (needed for appropriate conversion to energy units of kcal/mol (Nemethy *et al.*, 1992)) at the modified residues introduced into ECEPP/3 database of amino-acid residues.

After adding the nonstandard residues to the ECEPP/3 database we searched for low energy conformations using the EDMC method. We carried out the same calculation in vacuum and in a water environment. The range of temperatures during Monte Carlo simulations was from 500 K to 10000 K. Two thousand conformations of each oxytocin analog in vacuum and two thousand in water solution were found. These conformations were used as an input data for dihedral angle $\chi 1$ distribution analysis in ECEPP/3 force field.

Table 3. Z–matrix with charges for nonstandard residue *p*-Me-Phe introduced to ECEPP/3 database

Atom		Bond		Angle		Dihedral	Charge
N	1						–0.60798
HN	1	1.000					0.29423
CA	1	1.453	2	114.999			0.00804
HA	1	1.090	1	107.265	2	119.4	0.11501
CB	3	1.530	1	106.999	2	–118.8	–0.07839
C	3	1.530	1	111.000	2	0.0	0.07524
O	3	1.230	3	120.500	1	0.0	0.09663
HB	6	1.090	3	108.910	1	–58.2	–0.05192
HB	5	1.090	3	108.905	1	58.2	0.12109
CG	5	1.530	3	113.999	1	180.0	–0.17203
CD1	5	1.360	5	119.999	3	180.0	–0.03680
CD2	10	1.360	5	120.003	3	0.0	0.14541
HD1	10	1.090	10	120.000	5	0.0	–0.16631
CE1	11	1.420	10	119.998	5	180.0	–0.20301
CE2	11	1.420	10	120.003	5	180.0	0.06220
HD2	12	1.090	10	119.997	5	0.0	0.08380
HE1	12	1.090	11	119.999	10	180.0	0.06636
CZ	14	1.360	11	120.003	10	0.0	–0.12652
HE2	14	1.090	12	120.002	10	180.0	0.13258
CK	15	1.449	14	130.446	11	179.8	–0.18503
HK	18	1.088	18	109.391	14	–179.9	0.15138
HK	20	1.088	18	109.560	14	–59.9	0.51784
HK	20	1.089	18	109.380	14	60.2	–0.41403

RESULTS

Two thousand conformations of each oxytocin analog in two environments (vacuum or water) were taken into consideration during preparation of the angle distributions. In Fig. 1 the lowest energy members of each set of conformations are presented. Figure 2 shows the distribution of dihedral angle $\chi 1$ value in the modified residue [Phe^2] in the oxytocin analogs as a result of the ECEPP/3 calculations in water.

Figure 2a shows the distribution of the dihedral angle $\chi 1$ in the nonstandard amino-acid residue in [(Phe)^2*o*-Me]OT in water. Two sharply outlined maxima on the graph are readily noticeable. They are situated within the range: (–180°; –165°) and (–75°; –45°) and represent 38% and 57.7% of the whole angle population, respectively. The remaining area is occupied by just over 2% of the conformations. A similar situation is observed in the case of the calculations performed in vacuum (Fig. 3a). There are no significant shifts of the maxima of the preferred values in comparison with the first graph, except for some broadening of the maximum for the $\chi 1$ angle around 180° and appearance of a small maximum in the interval (–150°; –135°). The maxima are located in the intervals: (165°; –165°), (–150°; –135°) and (–75°; –45°) and represent 47.3%, 8.9% and 42.3% of the whole angle population, respectively.

Figures 2b and 3b show the distributions of the dihedral angle $\chi 1$ in the nonstandard amino-acid residue in [(Phe)^2*m*-Me]OT in water and in vacuum, respectively. As one can see, there are two distinct maxima in plot 2b: one in the range (–75°; –45°) comprising 68.4% of the population and the second occupying edges of the plot with 30% of the population. The first one practically overlaps analogous maxima of the distribution for *o*-methylphenylalanine in water (see Fig. 2a). The results obtained in vacuum suggest that most (82.5%) dihedral angle $\chi 1$ values are contained in the interval (–75°; –45°). The remaining conformations form the second distinct

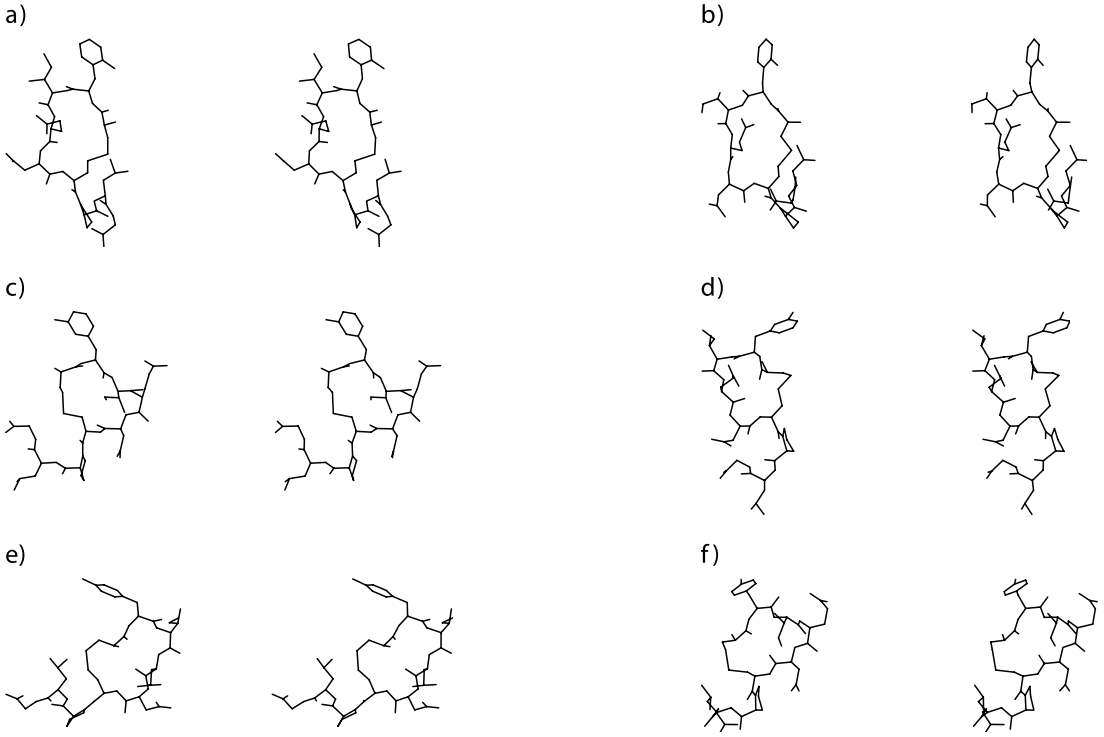

Figure 1. Stereoview of the lowest energy conformations of the considered analogs of oxytocin in vacuum and in water.

a) and b) [(Phe)^2*o*-Me]OT in water and in vacuum, respectively; c) and d) [(Phe)^2*m*-Me]OT in water and in vacuum, respectively; e) and f) [(Phe)^2*p*-Me]OT in water and in vacuum, respectively. All calculations were performed using EDMC method implemented in the ECEPP/3 force field. The lowest energy conformations were selected from two thousand conformations each of peptide in both environments.

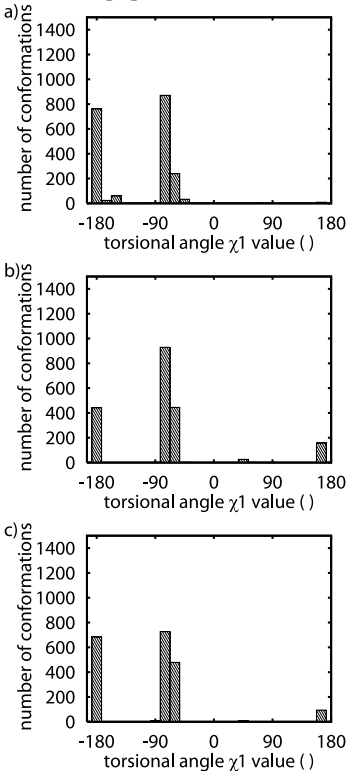

Figure 2. Distributions of the dihedral angle χ1 in methylphenylalanine in water.

a) [(Phe)^2*o*-Me]OT; b) [(Phe)^2*m*-Me]OT; c) [(Phe)^2*p*-Me]OT. The plots are drawn on the basis of the EDMC calculations in the ECEPP/3 force field using continuum solvent model.

maximum in the range (165°; –150°). Therefore the distribution is similar to the one of *o*-methylphenylalanine. The distributions of the dihedral angle χ1 in the nonstandard amino-acid residue in [(Phe)^2*p*-Me]OT are shown in Fig. 2c (water) and Fig. 3c (vacuum). The distribution in water is similar to the analogous distributions for the *ortho* and *para* isomers. Two sharply outlined maxima are placed in the ranges: (165°; –165°) and (–75°; –45°), representing 39.7% and 60.4% of the population, respectively. The distribution for structures calculated in vacuum is similar to the previous cases as well. There are two main maxima in the intervals: (–75°; –45°) and (165°; –165°), representing 18.8% and 73.1% of the population, respectively, a third, not so high in the interval (45°; 75°) representing 4.3% of the population. The distributions obtained from the vacuum calculations differ in the level of occupation of the particular interval. In the case of the distributions obtained from the calculations in the water, the populations of the conformations were divided quite evenly between two intervals, whereas the situation for vacuum looks as follow: conformations with the *meta* isomer prefer interval around –60° (82% of all conformations), conformations with the *para* isomer grouped in this interval constitute only 18.8% of the whole population, and conformations with the *ortho* isomer do not prefer distinctly either of the two intervals.

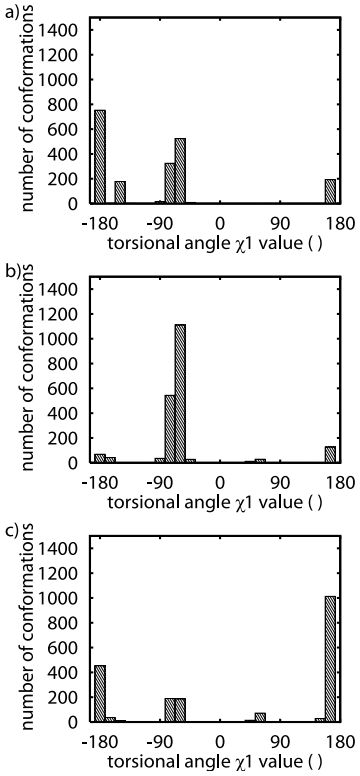

Figure 3. The distributions of the dihedral angle χ1 in methylphenylalanine in vacuum.
a) [(Phe)^2*o*-Me]OT; b) [(Phe)^2*m*-Me]OT; c) [(Phe)^2*p*-Me]OT. The plots are drawn on the basis of the EDMC calculations in the ECEPP/3 force field in vacuum environment.

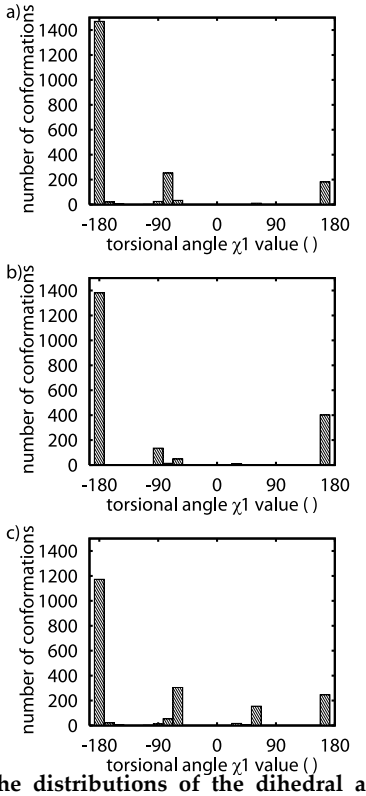

Figure 4. The distributions of the dihedral angle χ1 in amino-acid residue at position 8 in vacuum.
a) for [(Phe)^2*o*-Me]OT; b) for [(Phe)^2*m*-Me]OT; c) and for [(Phe)^2*p*-Me]OT. The plots are drawn on the basis of the EDMC calculations in the ECEPP/3 force field using continuum solvent model.

The distributions of the torsional angle χ1 for residue 8 in water (Fig. 4) are very consistent and individual plots do not differ significantly from each other. The placement of the methyl group in the phenyl ring of residue 2 does not appear to influence the spatial arrangement associated with the changes of χ1 value of the residue 8 side chain. The maxima of the plots are placed within the same regions: the first (greater) within the interval (165°; –165°) and the second (smaller) within the interval (–90°; 45°). The global maximum contains 82.4% of all conformations for the *ortho* isomer, 88.9% for *meta* and 70.85% for the *para* one. All the remaining conformers are confined to the second maximum. The preferred intervals overlap those found for residue 2.

In vacuum another maximum appears for isomers *meta* and *para* in the range of (–105°; –60°). It is present along side the two intervals known from the former distributions (see Fig. 5) There occur two main maxima — at (165°, –150°) and around –90° — on all three plots. The first interval contains 91.6%, 25.1% and 39.7% of the population for the *ortho*, *meta* and *para* isomers, respectively. The second interval contains 7.93%, 61.8% and 55.9% of all conformations of the corresponding analogs. These intervals overlap those from the other distributions.

Differences occur in the level of occupation of the intervals considered. The situation is very similar for the plots of distributions for isomers *meta* and *para* (Fig. 5b and 5c). More than half of all conformations is located in the interval around –90°. In the case of isomer *para* only 7.9% of all conformations prefer this region.

DISCUSSION

The torsional angle χ1 at residues 2 and 8 in free oxytocin analogs shows a strong tendency to adopt values from strictly defined, narrow intervals. The intervals preferred by the χ1 angle values at residue 2 in all three analogs seem to be independent of the environment (vacuum or water solution). This observation agrees with the fact that angle χ1 in peptides, generally, adopts one of three rotameric states: *gauche*(+), *trans* or *gauche*(–) (Marcus *et al.*, 1996; Bhargavi *et al.*, 2003). It is interesting to note that the conformation *gauche*(–) is practically absent on all plots. Nevertheless the level of the particular interval occupation seems to be dependent on both the environment and the MePhe isomer substituted in position 2 of oxytocin analog. This can be easily observed in the distributions from the simulations in vacuum environment (Fig. 3). Individual rotameric states are preferred with a different affinity by the individual analogs. The analog containing the *ortho*

Table 4. Character of the biological activity of individual analogs of oxytocin

Isomer	Mg^{2+} absence	Mg^{2+} presence
ortho	antagonist	agonist
meta	antagonist	antagonist
para	agonist	agonist

isomer prefers both occupied rotameric states approximately equally. The analog with the *meta* isomer evidently favors conformation *gauche(+)*, whereas the analog containing the *para* isomer clearly prefers the *trans* conformation. The character of the biological activity of the peptides considered in this paper is presented below (Slaninova *et al*., 2001):

If one attempts to arrange the individual analogs according to their growing agonistic properties depending on magnesium presence, the following order results:
[(Phe)^2*m*-Me]OT (always anatagonist) → [(Phe)^2*m*-Me]OT → [(Phe)^2*m*-Me]OT (always agonist).

We can easily notice that this sequence follows the growing tendency to adopt conformation *trans* by the angle $\chi1$ in residue 2 in the individual analogs:
[(Phe)^2*m*-Me]OT (17.5%) → [(Phe)^2*o*-Me]OT (47.3%) → [(Phe)^2*p*-Me]OT (73.1%).

Apparently, adoption of the *trans* conformation by angle $\chi1$ in residue 2 is correlated with the agonistic properties of the peptide and analogously adoption of the *gauche*(+) conformation can be correlated with antagonistic properties.

Moreover, the placement of the methyl group in the phenyl ring of the second residue seems to influence the side chain conformation of residue 8, which is believed to be correlated with the antagonistic activity of the oxytocin analogs (Bankowski *et al*., 1980; Manning *et al*., 1984; 1995; Hruby *et al*., 1994). This phenomenon is most clearly seen in the vacuum environment. If one arranges the individual plots according to the growing contributions of the *trans* conformers into the overall $\chi1$ angle distribution, the following order will be obtained:
[(Phe)^2*m*-Me]OT (25.1%) → [(Phe)^2*p*-Me]OT (39.7%) → [(Phe)^2*o*-Me]OT (91.6%).

It is not identical with the sequence observed in the case of residue 2, but we can conclude that the antagonistic properties can be correlated with the adoption of the *gauche*(+) conformation by angle $\chi1$ in residue 8.

Summarizing, the conformations *gauche*(–) seems to be very unfavorable in all considered analogs and residues. The agonistic properties of the peptides can be correlated with the adoption of conformation *trans* by the angle $\chi1$ in residue 2, whereas agonistic properties can be correlated with the adoption of conformation *gauche*(+) by the angle $\chi1$ in residue 8.

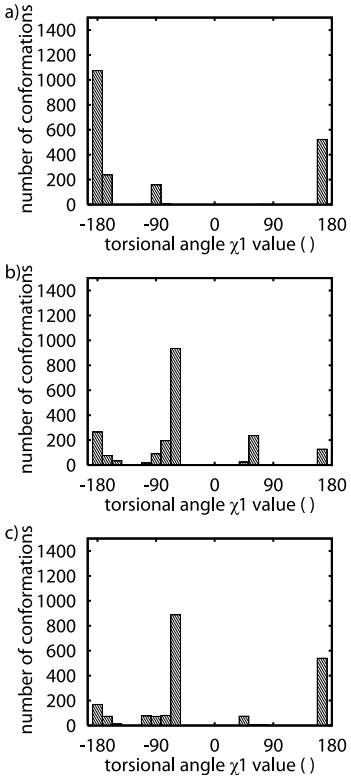

Figure 5. The distributions of the dihedral angle $\chi1$ in amino-acid residue at position 8 in solvent.
a) for [(Phe)^2*o*-Me]OT; b) for [(Phe)^2*m*-Me]OT; c) and for [(Phe)^2*p*-Me]OT. The plots are drawn on the basis of the EDMC calculations in the ECEPP/3 force field in vacuum environment.

Acknowledgements

This work was partially supported by grants BW/8000-5-0181-4 and KBN 0863/T09/2002/22.

REFERENCES

Bankowski K, Manning M, Seto J, Haldar J, Sawyer WH (1980) Design and synthesis of potent in vivo antagonists of oxytocin. *J Pept Protein Res* **16**: 382–391.

Barberis C, Mouillac B, Durroux T (1998) Structural bases of vasopressin/oxytocin receptor function. *J Endocrinol* **156**: 223–229.

Bhargavi GR, Sheik SS, Velmurugan D, Sekar K (2003) Side-chain conformation angles of amino acids: effect of temperature factor cut-off. *J Struct Biol* **143**: 181–184.

Bingham RC, Dewar MJS, Lo DH (1975) Ground states of molecules. XXV. MINDO/3. An improved version of the MINDO semiempirical SCF-MO method. *J Am Chem Soc* **97**: 1285–1293.

Budesinsky M, Prochazka Z, Slaninova J (2005) Oxytocin and its analogs, methyl-substituted in ortho-, meta- or para- position of aromatic ring of phenylalanine in position 2: NMR study and biological activities. *Protein Pept Lett* **12**: 343–347.

Burgess AW, McGuire RF, Momany FA, Scheraga HA (1975) Energy parameters in polypeptides. VII. Geometric parameters, partial atomic charges, non-bonded interactions, hydrogen bonded interactions, and intrinsic torsional potentials for the naturally occurring amino acids. *J Phys Chem* **79**: 2361–2381.

Higby K, Suiter CR (1999) A risk-benefit assessment of therapies for premature labour. *Drug Safety* **21**: 35–56.

Hruby VJ, Chan WY, Rockway TW, Hlavacek J, Ormberg J (1994) Design and synthesis of long-acting oxytocin anatagonists substituted in positions 2, 7, and 8. In *Peptides: Design, Synthesis and Biological Activity* (Basava C, Anantharamaiah GM, eds) vol 1, pp 198–208, Birkhauser Verlag, Boston.

Law D, Vigneaud VD (1960) Synthesis of 2-p-methoxyphenylalanine oxytocin (O-methyl-oxytocin) and some observations on its pharmacological behaviour. *J Am Chem Soc* **82**: 4579–4581.

Manning M, Nawrocka E, Misicka A, Olma A, Klis WA, Seto J, Sawyer WH (1984) Potent and selective antagonists of the antidiuretic responses to arginine-vasopressin based on modifications of [1-(beta-mercapto-beta,beta-pentamethylenepropionic acid),2-D-isoleucine, 4-valine]arginine-vasopressin at position 4. *J Med Chem* **27**: 423–429.

Manning M, Cheng LL, Stoev S, Bankowski K, Przybylski J, Klis WA, Sawyer WH, Wo NC, Chan WY (1995) An exploration of the effects of L- and D-tetrahydroisoquinoline-3-carboxylic acid substitutions at positions 2, 3 and 7 in cyclic and linear antagonists of vasopressin and oxytocin and at position 3 in arginine vasopressin. *J Pept Sci* **1**: 66–79.

Marcus E, Keller DA, Shibata M, Ornstein RL, Rein R (1996) Comparing theoretical and experimental backbone-dependent sidechain conformational preferences for linear, branched, aromatic and polar residues. *Chemical Physics* **204**: 157–171.

Nemethy G, Pottle MS, Scheraga HA (1983) Energy paramters in polypeptides. 9. Updating of geometrical parameters, non-bonding interactions and hydrogen bonding interactions for naturally occuring amino acids. *J Phys Chem* **87**: 1883–1887.

Nemethy G, Gibson KD, Palmer KA, Yoon CN, Paterlini G, Zagari A, Rumsey S, Scheraga HA (1992) Improved geometrical parameters and nonbonded interactions to use in the ECEPP/3 algorithms, with applications to proline-containing peptides. *J Phys Chem* **96**: 6472–6484.

Pearlman DA, Case DA, Caldwell JW, Ross WS, T. E. Cheatham III TE, DeBolt S, Ferguson D, Seibel G, Kollman P (1995) AMBER, a package of computer programs for applying molecular mechanics, normal mode analysis, molecular dynamics and free energy calculations to simulate the structural and energetic properties of molecules. *Comp Phys Commun* **91**: 1–41.

Schaftenaar G, Noordik JH (2000) Molden: a pre- and post-processing program for molecular and electronic structures. *J Comput-Aided Mol Design* **14**: 123–134.

Slaninova J, Maletinska L, Vondrasek J, Zertova M, Prochazka J (2001) Magnesium and biological activity of oxytocin analogs modified on aromatic ring of amino acid in position 2. *J Pept Sci* **7**: 413–424.

Toth GK, Bakos K, Penke B, Pavo I, Varga C, Torok G, Peter A, Fulop F (1999) Synthesis of oxytocin antagonists containing conformationally constrained amino acids in position 2. *Bioorg Med Chem Lett* **9**: 667–672.

Urry DW, Ohnishi M, Walter R (1970) Secondary structure of the cyclic moiety of the peptide hormone oxytocin and its deamino analog. *Proc Natl Acad Sci USA* **66**: 111–116.

Wood SP, Tickle IJ, Treharne AM, Pitts JE, Mascarenhas Y, Li JY, Husain J, Cooper S, Blundell TL, Hruby VJ, Buku A, Fischman AJ, Wyssbrod HR (1986) Crystal structure analysis of deamino-oxytocin: conformational flexibility and receptor binding. *Science* **232**: 633–636.

Wyatt PG, Allen MJ, Chilcot J, Hickin G, Miller ND, Woollard PM (2001) Structure-activity relationship investigations of a potent and selective benzodiazepine oxytocin antagonist. *Bioorg Med Chem Lett* **11**: 1301–1305.